Received: 16 October 2021 | Accepted: 25 August 2022

DOI: 10.1111/mms.12982

ARTICLE

Marine Mammal Science

Estimating body mass of sperm whales from aerial photographs

Maria Glarou[1,2,3] | Shane Gero[1,4] | Alexandros Frantzis[5] | José María Brotons[6] | Fabien Vivier[7] | Paraskevi Alexiadou[5] | Margalida Cerdà[6] | Enrico Pirotta[8,9] | Fredrik Christiansen[1,10]

[1]Zoophysiology, Department of Biology, Aarhus University, Aarhus, Denmark

[2]Department of Ecology, Environment and Plant Sciences, Stockholm University, Stockholm, Sweden

[3]Húsavík Research Centre, University of Iceland, Húsavík, Iceland

[4]Department of Biology, Carleton University, Canada

[5]Pelagos Cetacean Research Institute, Vouliagmeni, Greece

[6]Asociación Tursiops, Palma de Mallorca, Balearic Islands, Spain

[7]Marine Mammal Research Program, Hawai'i Institute of Marine Biology, University of Hawai'i at Mānoa, Kaneohe, Hawaii

[8]Centre for Research into Ecological and Environmental Modelling, University of St Andrews, St Andrews, UK

[9]School of Biological, Earth and Environmental Sciences, University College Cork, Cork, Ireland

[10]Aarhus Institute of Advanced Studies, Aarhus, Denmark

Correspondence
Maria Glarou, Hafnarstétt 3, Húsavík Research Centre, University of Iceland, 640 Húsavík, Iceland.
Email: mag133@hi.is

Abstract

Body mass is a fundamental feature of animal physiology. Although sperm whales (*Physeter macrocephalus*) are the largest toothed predators on earth, body mass is seldom included in studies of their ecophysiology and bioenergetics due to the inherent difficulties of obtaining direct measurements. We used UAV-photogrammetry to estimate the weight of free-ranging sperm whales. Aerial photographs (23 calves, 11 juveniles, 55 nonmother adults, 13 mothers) were collected in the Eastern Caribbean and Mediterranean Sea during 2017–2020. Body length, widths, and heights (dorso-ventral distance at 5% increments) were measured from dorsal and lateral photographs, while body volume was calculated using an elliptical model. Volume varied noticeably (12.01 ± 4.79 m^3) in larger animals (>8 m), indicating fluctuations in body condition of adults and mothers. Volume was converted to mass, using tissue-density estimates from catch data, animal-borne tags, and body-tissue composition. Average total body density ranged from 834 to 1,003 kg/m^3, while the weight predictions matched with existing measurements and weight-length relationships. Our body-mass models can be used to study sperm whale bioenergetics, including inter- and intraseasonal

Funding information
Arizona Center for Nature Conservation; Carlsbergfondet; Dansk Akustisks Selskab; Dansk Tennis Fond; Det Frie Forskningsråd; Erasmus+ Programme; Focused on Nature; Fundación Biodiversidad of the Ministerio para la Transición Ecológica y Reto Demográfico of the Gobierno de España; National Geographic Society; OceanCare; Oticon Fonden; Quarters For Conservation; University of Manchester; Villum Fonden

variations in body condition, somatic growth, metabolic rates, and cost of reproduction.

KEYWORDS
body condition, marine mammal, morphometrics, odontocete, *Physeter macrocephalus*, unmanned aerial vehicle

1 | INTRODUCTION

Body mass is a fundamental feature of animal physiology and contributes significantly to shaping animal ecology and behavior (Calder, 1982; Schmidt-Nielsen, 1984). Among other factors, body mass influences metabolic rates and caloric needs (Kleiber, 1947), growth (Calder, 1982), thermoregulation (Porter & Kearney, 2009), the aerobic dive limit (ADL; Kooyman et al., 1981) and home range (McNab, 1963). Whales are the largest animals on the planet (Goldbogen et al., 2019), and due to their size, play important ecosystem roles (Lavery et al., 2010; Roman et al., 2014; Roman & McCarthy, 2010; Smith, 2007). Despite this, body mass is seldom included as a variable in studies of large whales, due to the challenge of accurately measuring body mass in free-ranging individuals.

Sperm whales (*Physeter macrocephalus*, Linnaeus 1758) are the largest extant odontocetes (i.e., toothed whales) and the largest toothed predators on the planet (Cantor et al., 2019). Females typically reach about 11 m in body length in oceanic populations and can weigh up to 15,000 kg, while males commonly reach about 16 m and can weigh up to 45,000 kg (Rice, 1989). Much larger males, up to about 20 m, have been recorded in the past (McClain et al., 2015). The species was subject to heavy exploitation during the whaling era, with approximately two-thirds of the global population being killed for commercial purposes (Whitehead, 2002). Despite this dramatic decline in their numbers, sperm whales remain important ecosystem engineers (Roman et al., 2014), consuming around 100 megatons of biomass annually (Whitehead, 2003). Using a powerful biosonar, they are able to echolocate and catch their prey in the dark deep-sea environment (Miller et al., 2004a; Tønnesen et al., 2020; Watwood et al., 2006), thus playing a vital role in deep-sea energy turnover (Lavery et al., 2010). The large body size of sperm whales enhances their diving capacity (Watwood et al., 2006), while their hyper-scaled biosonar improves prey detection range (Goldbogen & Madsen, 2018; Jensen et al., 2018). With long breath-hold times and augmented prey detection abilities, sperm whales can optimize their foraging strategies and increase their dive-specific energy intake by remaining longer at depth and therefore catching additional prey than if they had shorter dives (Goldbogen et al., 2019; Rice, 1989). Their large size is also correlated with low mass-specific metabolic rates, which allow for increased energy storage due to a decrease in energy expenditure (Irvine et al., 2017; Lockyer, 1981). Using these energy stores combined with concurrent intake of exogenous resources, sperm whales are able to support their energetically costly reproduction (Lockyer, 1981; Soulsbury, 2019; Stephens et al., 2009) and endure long-range displacements (Clarke, 1972).

Although large body size is an important characteristic of sperm whales, the role of body mass is often understudied due to the inherent difficulties of obtaining measurements from free-ranging individuals. Existing data on sperm whale body mass are limited, and originate either from historical catch records (Gambell, 1970; Lockyer, 1976, 1991; Ohno & Fujino, 1950; Omura, 1950; Tomilin, 1967) or stranded animals (Jauniaux et al., 1998). Several studies include weight-length relationships of caught sperm whales (Lockyer, 1976, 1991; Omura, 1950) based on which body mass can be predicted from body length, albeit none of those models accounted for fluctuations in girth (i.e., body volume), which may reflect changes in the lipid-store body condition of individuals. Body condition is a measure of the relative energy reserves of an animal and may be used to assess individual fitness, survival, and reproductive success, as well as reflect the effects of disturbance or resource depletion on vulnerable populations (Booth et al., 2020; Castrillon & Bengtson Nash, 2020; Christiansen et al., 2018, Christiansen et al., 2020a;

Christiansen et al., 2021; Peig & Green, 2010; Stevenson & Woods, 2006). This metric is often expressed as the body mass, volume, girth, or width in relation to body length (the structural size of the animal) or as the residual of the regression between them (Green, 2001; Jakob et al., 1996; Moya-Laraño et al., 2008; Stevenson & Woods, 2006). Only a handful of existing studies account for variation in body condition, as they include estimates of body mass from volume (i.e., girth and length) (Bose et al., 1990; Sleet et al., 1981) or quantify the variation in blubber thickness and lipid content with length (Evans et al., 2003); however, those refer to sperm whales that were involved in stranding incidents. Evidently, obtaining measurements from dead specimens (stranded or caught) comes with certain constraints (Moore & Read, 2008) or ethical concerns (Aron et al., 2000). For instance, there is a lot of uncertainty around body-mass data of caught whales, as these measurements typically originate from whales weighed in parts and may not account for the loss of fluids that occurs during flensing (Lockyer, 1976). Similarly, measurements from stranded animals may not be representative of a healthy population (Barratclough et al., 2014; Currie et al., 2021; Moore et al., 2004). Hence, it is essential to develop a noninvasive method to estimate body mass of free-ranging sperm whales, while also accounting for variation in their body condition.

The aim of the present study was to estimate the body mass of free-ranging sperm whales. First, we used noninvasive UAV photogrammetry methods (Christiansen et al., 2016, 2019) to obtain morphometric measurements of sperm whale body shape, including body length, width (lateral distance), and height (dorso-ventral distance). From these measurements, we estimated the body volume of the whales and then converted volume to mass using published estimates of sperm whale body tissue density derived from different sources, including catch data, animal-borne tags, and body tissue composition. Given their crucial role in deep-sea energy turnover, as well as their threatened conservation status (Gero & Whitehead, 2016; Notarbartolo di Sciara et al., 2012; Taylor et al., 2019), information on body weight of sperm whales is essential and provides a valuable insight into their ecophysiology and bioenergetics.

2 | METHODS

2.1 | Data collection

Aerial videos and photographs of sperm whales were collected between 2017 and 2020 in the Eastern Caribbean Sea (Dominica) and the Mediterranean Sea (Balearic Islands, Spain, and Hellenic Trench, Greece) using two different UAV setups (Table 1). The first UAV setup included a DJI Inspire 1 Pro quadcopter (56 cm diameter, 3.4 kg, https://www.dji.com), equipped with an Olympus M.Zuiko 25 mm f1.8 lens mounted on a 16-megapixel DJI Zenmuse X5 micro four-thirds camera, while the second UAV setup included a DJI Phantom 4 Pro quadcopter (35 cm diameter, weight = 1.368 kg, https://www.dji.com). For the purpose of scaling the images, a LightWare SF11/C laser rangefinder (Lightware Optoelectronics, weight: 35 g) was attached to the UAVs to determine the flight altitude above sea level, or the images were scaled using the length of a known object depending on the location and sampling season (Table 1). During data collection, the UAVs were flown from a research vessel at altitudes ranging from 12.9 to 96.7 m ($M = 33.7$ m, $SD = 17.1$ m), and, when recording or photographing a sperm whale, the camera was stabilized

TABLE 1 Summary table of sampling periods, UAV models and scaling method used in each sampling location.

Location	Sampling period	UAV model	Scaling method
Dominica	2017–2018	DJI Inspire 1 Pro	Laser rangefinder
Balearic Islands	2020	DJI Phantom 4 Pro	Known-sized object
Greece	2019	DJI Phantom 4 Pro	Laser rangefinder
Greece	2020	DJI Inspire 1 Pro	Laser rangefinder

and angled vertically (90°) by a gimbal. To minimize radial distortion cause by the lens properties, the whales were always kept in the center of the frame where the effects of lens distortion are minimal (Burnett et al., 2019). In addition to the UAV data, DSLR cameras were used onboard to take fluke or dorsal fin area photographs of the sperm whales for the purpose of identifying different individuals (Arnbom, 1987; Frantzis et al., 2014; Whitehead & Gordon, 1986).

2.2 | Morphometric measurements

High-resolution still images were extracted from the UAV video recordings post hoc. Still images and photographs in which the whales were lying flat (i.e., nonarching) at the surface and were displaying their dorsal side were selected to measure the total body length (*BL*, distance from tip of rostrum to the end of fluke notch) and the body width (*W*) at 5% intervals along the body axis (Christiansen et al., 2016; Figure 1A). Similarly, images in which the whales were displaying their lateral side were used to measure the body height (*H*, dorso-ventral distance) at the same 5% intervals as the width measurements (Christiansen et al., 2019; Figure 1B). All photogrammetric measurements (in pixels) were performed in R v4.0.5 (R Development Core Team, 2018) using a custom-built script (Christiansen et al., 2016).

To convert (scale) the pixel measurements to distance measurements (in meters), two different methods were used depending on the UAV setup. Aerial images collected from Dominica and the Hellenic Trench were linked to the rangefinder altitude measurements during postprocessing, to determine the UAV altitude above sea level. Following the methods of Christiansen et al. (2018), the body length (*BL*) of whale *i* was calculated by Equation 1:

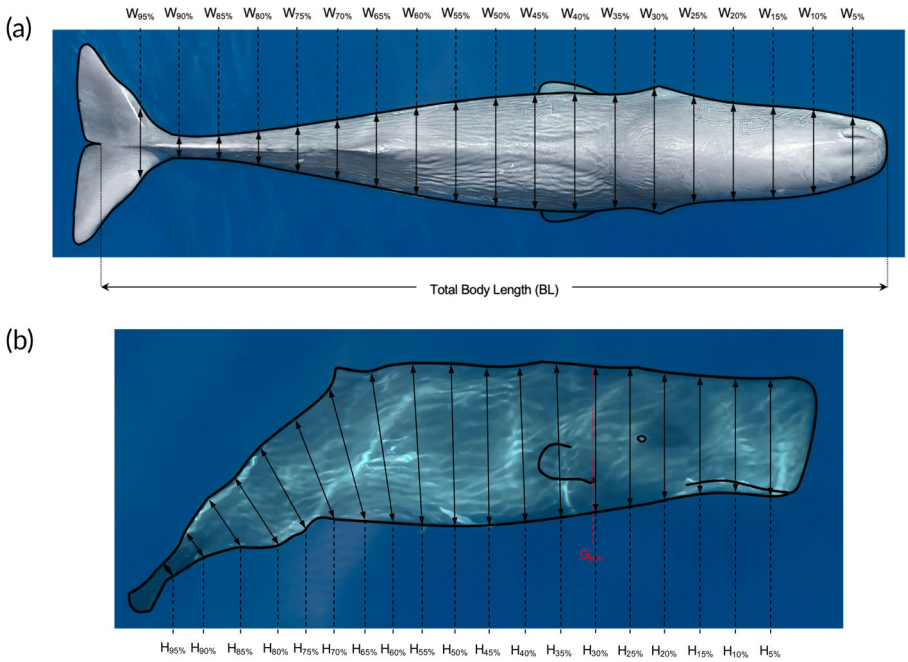

FIGURE 1 (a) Aerial image of the dorsal view of a sperm whale, along with the schematic depiction of all measurement sites. We measured the total body length (*BL*) and the body width (*W*) at 5% increments along the body axis. (b) Aerial image of the lateral view of a sperm whale, used to extract body height measurements (*H*, dorso-ventral distance) at 5% increments along the body axis. The location of the estimated body girth (G_{pec}, at 31% *BL* from the rostrum) is indicated by the red dotted line in the schematic depiction.

$$BL_{i,\mathrm{m}} = \frac{BL_{i,\mathrm{pix}}}{\frac{\text{image width resolution}_{\mathrm{pix}}}{\text{sensor width}_{\mathrm{mm}}}} \times \frac{\text{altitude}_{i,\mathrm{m}}}{\text{focal length}_{\mathrm{mm}}}. \quad (1)$$

Aerial images collected from the Balearic Islands were scaled using the length of a known object (i.e., the boat canopy), following the methods of Christiansen et al. (2016). Thus, for the purpose of scaling a sperm whale, the boat canopy was always photographed with the UAV, either in the same frame as the whale or from the same altitude as the last image of the whale. The altitude of the boat canopy above sea level was accounted for in the scaling calculations.

All selected images were quality-rated based on clarity, contrast and whale posture following the criteria set by Christiansen et al. (2018). Each image was rated with a score from 1 (good quality) to 3 (poor quality) for each of the following attributes: camera focus, body straightness (horizontally), body pitch (vertically), degree of body roll, degree of body arch, body length measurability, and body width measurability (Christiansen et al., 2018). Only photographs of adequate quality (scores 1 and 2) were included in the final data set. Vessel-derived fluke and dorsal fin area photographs were used to identify each whale that was measured in the study, and repeated measurements from the same individuals taken within the same day, were removed to avoid pseudoreplication. Lastly, all individuals were assigned to a specific reproductive class: calf, juvenile, adult, and mother. Mothers and calves were classified based on monitoring data that indicated a close association to each other over repeated encounters (Gero et al., 2014). For the remaining individuals, classification into juveniles and adults was based on body-length thresholds derived from the largest calf and smallest mother measured in this study, specific to each area (Table S1). In the Caribbean Sea, sperm whales measuring less than 7.3 m were classified as calves, while individuals measuring more than 8.3 m were classified as adults. In the Mediterranean Sea, individuals measuring less than 5.7 m were classified as calves, while individuals measuring more than 7.5 m were classified as adults (Table S1). Lastly, animals with total length between these thresholds were classified as juveniles (Table S1). The age class thresholds in this study fall closely within previously defined length boundaries for sperm whales (Clarke et al., 2011; Frantzis et al., 2014; Nishiwaki et al., 1963).

2.3 | Body shape, volume, and condition

Assuming an elliptical cross-sectional body shape, the body volume (V) of the whales was estimated using the length, width, and height measurements from the UAV data, following the approach of Christiansen et al. (2019). To model the body shape of sperm whales, we first calculated the height to width (HW) ratio at each measurement site for the seven individuals of which their lateral side was captured (Figure 1a, b). Using the mean HW ratios for each measurement site, we then predicted H from W for the whales that had only been photographed displaying their dorsal side. Each 5% body segment s was then modeled as a series of infinitesimal ellipses, and the volume V of each segment s of whale i was calculated using the equation of Christiansen et al. (2019):

$$V_{s,i} = BL_i \times 0.05 \times$$

$$\int_0^1 \pi \times \frac{W_{A,s,i} + (W_{P,s,i} - W_{A,s,i}) \times x}{2} \times \frac{H_{A,s,i} + (H_{P,s,i} - H_{A,s,i}) \times x}{2} dx, \quad (2)$$

where BL_i is the total body length of individual i and, $W_{A,s,i}$, $H_{A,s,i}$, and $W_{P,s,i}$, $H_{P,s,i}$ are the anterior and posterior width and height (predicted) measurements of body segment s of individual i respectively. The total body volume $V_{tot,i}$ of an individual i was calculated as the sum of the volume $V_{s,i}$ of all body segments ($s = 20$) (for details, see Christiansen et al., 2019):

$$V_{\text{tot},i} = \sum_{s=1}^{20} V_{s,i}. \tag{3}$$

The relationship between body volume and body length was investigated using linear models. Both variables were log-transformed to account for the curvilinear relationship between volume and length.

A relative index of body condition (BC_i) of sperm whales was calculated from the residual of the relationship between body volume and length (Christiansen et al., 2020a; Christiansen et al., 2020b; Christiansen et al., 2021):

$$BC_i = \frac{BV_{\text{obs},i} - BV_{\text{exp},i}}{BV_{\text{exp},i}}, \tag{4}$$

where $BV_{\text{obs},i}$ is the observed body volume of whale i (in cubic meters) and $BV_{\text{exp},i}$ is the expected (or predicted) body volume of whale i (in cubic meters) given by the linear relationship between body volume and length on the log–log scale. Positive body condition values indicate that an individual is in relatively better body condition than an average individual of the same body length, whereas negative values indicate poorer body condition than average.

To investigate whether the variation in lung volume during gas exchange was visible morphologically (i.e., influencing body volume), we selected five individuals for which the respiration sequence was filmed under calm sea state conditions, and we extracted a series of still images before, during, and after gas exchange. For each sperm whale, we extracted 11 dorsal images (at 1 s intervals) starting at the 5 s mark before exhalation, then at the moment of the exhalation, and ending at the 5 s mark after exhalation. The subsequent inhalation always occurred within 1 or 2 s after exhalation, and thus, the 5 s time frame was sufficient to capture any morphometric changes that may have been visible. The width at 40% *BL* from the rostrum, relative to *BL*, was deemed representative of the lung position (Jiang et al., 2021), and was measured using the same custom-built R script as for the full morphometric measurements (Christiansen et al., 2016). The potential influence of gas exchange on the body width was investigated using a generalized additive mixed model (GAMM), with the relative width-to-length measurement at 40% *BL* from rostrum as the response variable, the time interval as the explanatory variable, and the individual as a random effect.

2.4 | Converting body volume to body mass

2.4.1 | Estimating sperm whale body density from whaling records

Few studies provide body weight measurements of sperm whales (Gambell, 1970; Lockyer, 1976, 1991; Ohno & Fujino, 1950; Omura, 1950; Tomilin, 1967). Of those, only Lockyer (1991) included measurements of length, girth and mass, which are essential for relating volume to body mass (Christiansen et al., 2019). Those measurements derived from three sperm whales caught off Durban, South Africa between March 4 and 12, 1973 (Lockyer, 1991). Two of these whales were females (one calf and one adult) with body lengths of 4.60 m and 11.51 m, while the third one was a male calf with a body length of 4.22 m. Weight was measured to the nearest kilogram and length and girth were measured to the nearest centimeter. Girth measurements were taken from the anterior end of the pectoral fin of each caught whale, at ~31% *BL* from the rostrum (Lockyer, 1991).

To determine the body density of the caught sperm whales, we first used the height and width measurements of the free-ranging whales to calculate their circumference (i.e., girth) at the anterior end of the pectoral fin, G_{pec} (Figure 1b), using the following equation (Christiansen et al., 2019):

$$G_{\text{pec}} = 4 \times \int_0^{\frac{\pi}{2}} \sqrt{r_{w,\text{pec},i}^2 \times \cos(x)^2 + r_{H,\text{pec},i}^2 \times \sin(x)^2}\, dx, \tag{5}$$

where $r_{W,\text{pec},i}$ and $r_{H,\text{pec},i}$ represent the radius of the body width and height of whale i at the anterior end of the pectoral fin (~31% *BL*), respectively. Using linear models, the body volume (V) was then modeled as a function of total body length (BL) and girth (G_{pec}):

$$\log(V_i) = \alpha + \beta_1 \times \log(BL_i) + \beta_2 \times \log(G_{\text{pec},i}) + \varepsilon_i. \tag{6}$$

Using this linear model on the caught whales, along with the length and girth measurements from Lockyer (1991), we were able to predict their body volumes, similar to Christiansen et al. (2019). By dividing the body-mass measurements with the volume predictions, we calculated the tissue density of each caught specimen (Lockyer, 1991).

2.4.2 | Accounting for gas components

To account for the effect of air components on body volume and total body density, we used a correction factor on all approaches. For Models 2 and 3, the body density estimates were corrected to account for both tissue and gas components, using the mean air volume estimates of Miller et al. (2004b). The mean air volume in the sperm whale body was estimated to be 0.0000264 m^3/kg (Miller et al., 2004b), thus the volume of air, $V_{\text{gas},i}$ (in cubic meters), in living animals, can be calculated from Equation 7a, where $M_{\text{tissue},i}$ is the estimated weight (in kilograms) of 1 m^3 of tissue, based on the tissue density estimates for each approach i (see sections 2.4.1. and 2.4.3):

$$V_{\text{gas},i} = 0.0000264 \times M_{\text{tissue},i}. \tag{7a}$$

For Models 1 and 4, we assumed that compression would greatly reduce the air components in intact corpses, compared to a living animal. Empirical observations from the whaling era indicate that the lungs were almost completely empty in dead large whales (Laurie, 1933). Although, to our knowledge, no quantitative estimates exist on how much air is left in the lungs after killing a sperm whale, we hypothesized that the residual gas would be approximately 10% of that of a living animal. Our hypothesis was based on tidal volume estimates of smaller cetaceans, which can reach approximately 80%–90% of the total lung capacity (Irving et al., 1941; Olsen et al., 1969), as well as the allometric relationship between tidal volume and body mass (Villegas-Amtmann et al., 2015), which provided a mean tidal volume of 95% of the total lung capacity for the three caught animals. However, the mean tidal volume of 95% is slightly overestimated, as the mass measurements from Lockyer (1991) used in the allometric relationship did not account for the weight of the missing gas components. Thus, our hypothesis of 10% residual gas in the lungs is likely a reasonable estimate.

Based on these assumptions, we first subtracted 90% of the mean air volume estimate (representing the air that left the body after death) from the total body volume estimates of the three caught sperm whales, and subsequently we divided their mass measurements with the new body volume estimates to calculate the tissue density. The total body density estimates of the dead whales included the tissue density and the density of residual gases (10% of total air volume). We then used a modified version of Equation 7 to correct for the missing 90% of gas volume in our density estimates (Equation 7b):

$$V_{\text{gas},i} = 0.90 \times 0.0000264 \times M_{\text{tissue},i}. \tag{7b}$$

The weight of the gas components, $M_{gas,i}$ (in kilograms) of 1 m^3 of tissue, was calculated with Equation 8, where we multiplied the volume of gas with the air density at 1 atm, which equals to 1.225 kg/m^3:

$$M_{gas,i} = V_{gas,i} \times 1.225. \tag{8}$$

Lastly, to calculate the total tissue density (in kilograms per cubic meter) for each approach i, which accounted for both tissue and gas components, we used Equation 9:

$$D_{total,i} = \frac{M_{tissue,i} + M_{gas,i}}{1.0 + V_{gas,i}}. \tag{9}$$

2.4.3 | Estimating body mass of sperm whales

The mass, M, of whale i was determined using our elliptical body volume model, $V_{s,i}$, multiplied with the body density, D, of the whales. The body density (in kilograms per cubic meter) was calculated using four different approaches. For the first approach (Model 1), we assumed a uniform body composition, and calculated the mean body density, $D_{estimated}$, of a sperm whale using the derived density estimates from the three caught whales, adjusted to include gas components (see sections 2.4.1 and 2.4.2):

$$M_{Model1,i} = \sum_{s=1}^{S} V_{s,i} \times D_{estimated}. \tag{10}$$

For the second approach (Model 2), we used the published mean tissue density estimate for sperm whales derived from digital tags, D_{dtag} (Miller et al., 2004b), which we adjusted to include the density of gas components (see section 2.4.2). Miller et al. (2004b) first estimated the length of the tagged sperm whales using laser photogrammetry. Using a published weight-length relationship (Lockyer, 1976) adjusted for 25% fluid loss (Rice, 1989), Miller et al. (2004b) were then able to predict the weight of the tagged whales, and ultimately, estimate the mean tissue density using data from animal-borne tags:

$$M_{Model2,i} = \sum_{s}^{S} V_{s,i} \times D_{dtag}. \tag{11}$$

For the third approach (Model 3), we assumed a nonhomogenous body composition, as the body consists of several tissue types (blubber, muscle, bones, viscera). To account for these variations, we obtained the average body density of sperm whales, $D_{relative}$, using the relative proportions of each tissue type, combined with tissue-specific weights (Lockyer, 1976) and published tissue densities (grams per milliliter; Charrondiere et al., 2012; Lonati et al., 2019): (1) blubber accounts for 33% of body weight with a density of 0.87 g/ml (Lonati et al., 2019); (2) muscle accounts for 34% of body weight with a density of 0.96 g/ml; (3) bones account for 10% of body weight with a density of 0.72 g/ml; (4) visceral and organ tissue accounts for 9% of body weight with a density of 0.93 g/ml; and fluids comprise the remaining 14% of body weight with a density of 1.00 g/ml. The tissue density estimate from this approach was also adjusted to include gas components, similar to Model 2:

$$M_{Model3,i} = \sum_{s=1}^{S} V_{s,i} \times D_{relative}. \tag{12}$$

For the fourth approach (Model 4) we modeled the estimated total body density (tissue and gas) of the three caught whales as a function of body volume (Lockyer, 1991) to examine the effect of body size on body density, and obtained a volume-specific body density estimate, where $D_{i,\text{estimated}}$ is the density of whale i for a given body volume:

$$M_{\text{Model4},i} = \sum_{s=1}^{S} V_{s,i} \times D_{i,\text{estimated}}. \quad (13)$$

The relationship between predicted body mass M_i of individual i calculated using body density x, and body length BL_i was modelled for all approaches, using linear models:

$$\log(M_{x,i}) = \alpha + \beta \times \log(BL_i) + \varepsilon_i. \quad (14)$$

The resulting linear models were compared to four previously published mass-at-length relationships:

1. Omura (1950): Measurements from 13 sperm whales caught off Japan in the North Pacific Ocean, weighed in parts without accounting for fluid loss.
2. Lockyer (1976): Measurements from 47 sperm whales caught off Japan, Iceland, Canada Bering Sea and Antarctica, weighed in parts without accounting for fluid loss.
3. Lockyer (1991): Lockyer (1976)'s weight-length relationship, with weights adjusted for 10% fluid loss.
4. Lockyer (1976); Rice (1989): Lockyer (1976)'s weight-length relationship, with weights adjusted for 25% fluid loss (Rice, 1989).

The residual standard error for all linear models was plotted against body volume, reproductive class, body length, body condition, location, and sex.

2.5 | Model validation, UAV error assessment and sensitivity analysis

Model validation tests were run to ensure that all linear models met the necessary assumptions. We explored the homogeneity of variance with scatter plots of residuals against fitted values and against each explanatory variable. The normality of residuals was investigated through quantile−quantile plots and residual histograms. Influential points and outliers were checked through leverage and Cook's distance. All model assumptions were fulfilled.

All morphometric measurements taken by the UAV come with some uncertainty, due to errors associated with measurement precision and whale posture, the lens properties (particularly for the Phantom 4 Pro images) or the specific scaling method used (laser rangefinder versus known sized objects in the images). The mean measurement error for repeated measurements of the same animals within the same day for this method is between 3.11% and 4.75%, as quantified by Christiansen et al. (2018), who used a much larger sample size (1,118 photographs) than this study. Potential measurement errors resulting from the relative position of the whale in the image frame (e.g., higher lens distortion if positioned on the corners) for the Phantom 4 Pro images were investigated by plotting the body condition against the spatial coordinates (X and Y pixels) of the whale in the frame (Christiansen et al., 2016). In addition to that, to quantify the extent to which lens distortion potentially impacted our measurements, we compared the length and width (at 40% BL) of 8 sperm whales that were positioned at the edges of the image frame and compared the original and corrected images, using the distortion coefficients of Phantom 4 Pro (Burnett et al., 2019). Lastly, to investigate the effect of the measurement errors on the final models due to the scaling method used, a sensitivity analysis was run using resampling methods

(Christiansen et al., 2016, 2018). First, the error in body length estimation was quantified for the data originating from Dominica and the Hellenic Trench (both using laser rangefinder to scale measurements) and the data originating from the Balearic Islands (using a known sized object to scale images), using repeated measurements from the same individuals to calculate the standard deviations (*SD*) in body length estimates. One thousand bootstrap iterations were run, and during each iteration the body length was resampled for each individual from a Gaussian distribution of values, with a *SD* equal to the scaling error and the mean equal to the raw body length measurement. Additionally, the length measurability and width measurability scores (both part of the quality rating of images) were used to resample the resulting body length and body width measurements of the whales and assess the within-image precision (Christiansen et al., 2018). The following relationships were then reinvestigated using linear models: (1) body volume ~ body length, (2) body volume ~ body length + girth, (3) body density ~ body volume, and (4) body weight ~ body length. For each model, the model parameters were extracted. By doing this 1,000 times, we were able to obtain a density distribution of possible values for each model parameter, which we compared to the original model parameter. All four models were robust to scaling errors.

3 | RESULTS

3.1 | Sperm whale sample

In Dominica, data collection took place between April 5 and May 26, 2017 (10 days of sampling), and between May 18 and 25, 2018 (3 days of sampling). In the Balearic Islands, data were collected between May 11 and September 27, 2020 (27 days of sampling). In the Hellenic Trench, data collection was carried out between July 20 and August 10, 2019 (1 day of sampling) and between July 11 and August 22, 2020 (2 days of sampling). Because the methods of this study were not contingent on location, all collected data were pooled together for all further analyses. A total of 248 still images and photos of sperm whales displaying their dorsal side were extracted, and body length (*BL*) and width (*W*) measurements were obtained from all of them. Additionally, we selected 17 still images that fulfilled the quality grading criteria, in which the sperm whales displayed their lateral side. The lateral images were used to extract height (*H*) measurements relative to total length, in order to compare the lateral body shape of sperm whales between the three locations. Matching dorsal and lateral photos were obtained from seven individuals. In total, 138 images fulfilled the quality grading criteria and, after removing repeated measurements of the same individuals, a total of 102 images of individual sperm whales were included in the analyses. Of those, 23 were classified as calves (*BL* = 3.37–7.29 m; *M* = 5.64, *SD* = 1.08; Table S2), 11 as juveniles (*BL* = 5.78–8.26 m; *M* = 7.19, *SD* = 0.95; Table S2), 55 as adults (*BL* = 7.54–12.67 m; *M* = 9.70, *SD* = 1.50; Table S2) and 13 as mothers (*BL* = 7.56–9.98 m; *M* = 8.85, *SD* = 0.72; Table S2).

3.2 | Body shape, volume, and condition

The *HW* ratios were based on the seven sperm whales for which we obtained matching dorsal and lateral photos. This sample contained two calves and five adults. We compared the lateral body shape of sperm whales between the three locations using ANOVA for all measurement sites across *BL*, and we found no significant difference in the majority of measurement sites across the body (Table S3). Thus, we used the same mean *HW* ratios across our entire data set (Figure S1, Table S4). The cross-sectional body shape of sperm whales varied noticeably along the body axis (Figure 2). The *HW* ratio was always larger than one, suggesting a vertically elongated body shape throughout all segments (Figure 2, Table S4). This was especially pronounced towards the posterior end of the body, beyond ~60% *BL*

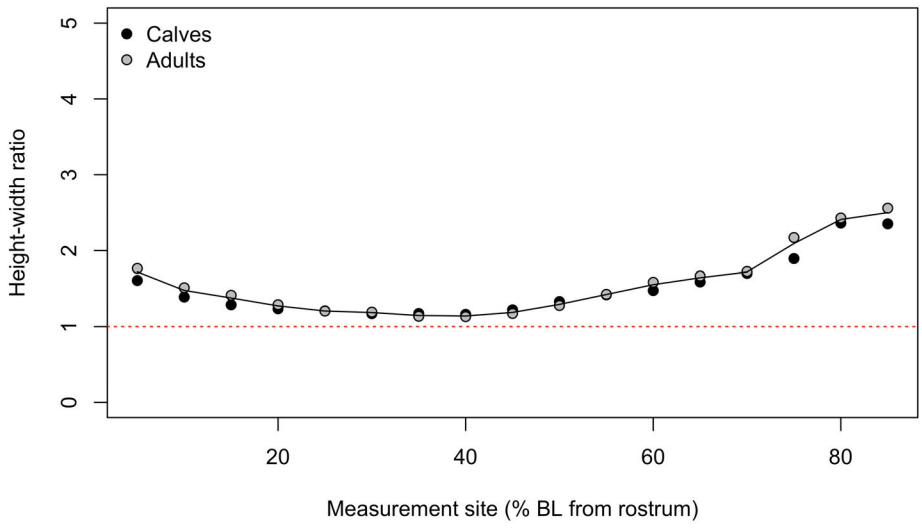

FIGURE 2 Height-to-width (*HW*) ratios of sperm whale calves ($n = 2$) and adults ($n = 5$) across the body. The ratio of 1:1 (where the height matches the width) is indicated by the dashed red line. The solid black line represents the mean *HW* ratios across all reproductive classes.

from the rostrum (Figure 2). The front part was also flattened in the lateral plane, albeit not as much as in the posterior end (Figure 2). In contrast, the shape of the middle part of the body (between ~25% *BL* and ~ 45% *BL*) approached a *HW* ratio of 1:1, which indicates an assumed circular body shape (Figure 2). Highest variation in body widths (relative to *BL*) across the body was observed around the dorsal fin area, between 50% and 65% *BL* from rostrum (Figure S2).

The linear model analysis showed a strong positive relationship between sperm whale body volume estimates and body length measurements on the log–log scale ($R^2 = 0.979$; Figure 3):

$$\log(V_i) = -4.048 + 2.861 \times \log(BL_i). \quad (15)$$

The body volume estimates of sperm whales in this study ranged from 0.59 to 24.36 m^3 ($M = 8.94$, $SD = 5.65$; Table S2). The estimated body volume varied noticeably (6.30–24.36 m^3; $M = 12.01$; $SD = 4.79$) in sperm whales over 8 m in length (Figure 3), indicating equivalent fluctuations in their relative body condition (−0.166–0.385; $M = 0.015$, $SD = 0.123$; Figure 4). In sperm whales smaller than 8 m in length, the estimated body volume ranged from 0.59 to 7.84 m^3 ($M = 3.77$; $SD = 2.09$), resulting in less variation in body condition (−0.201–0.178; $M = -0.011$; $SD = 0.097$; Figure 4).

We found that body width at 40% *BL* from rostrum (i.e., lung position), relative to *BL*, was not affected during the gas exchange sequence (GAMM, $F = 0.549$, $p = .462$; Figure 5). This indicates that any fluctuations in lung volume during respiration are not morphologically visible, and thus the time of image extraction (before, during or after a breath) has no influence on the body condition, volume, and mass estimates of this method. Further, there was no clear sign of spatial autocorrelation between the relative position of the whale in the frame and the body condition metric (Figure 3), lens distortion errors for the eight worst-positioned animals of our data set were <2.5% for width and length measurements and <3.5% for the width/length ratio.

The predicted girths at the anterior end of the pectoral fin (calculated from the *W* and predicted *H* data) ranged from 2.01 to 6.51 m ($M = 4.42$, $SD = 1.00$; Table S2). The linear model used to predict the volume of the caught sperm whales from *BL* and G_{pec} explained 99% of the variance (R^2) in body volume:

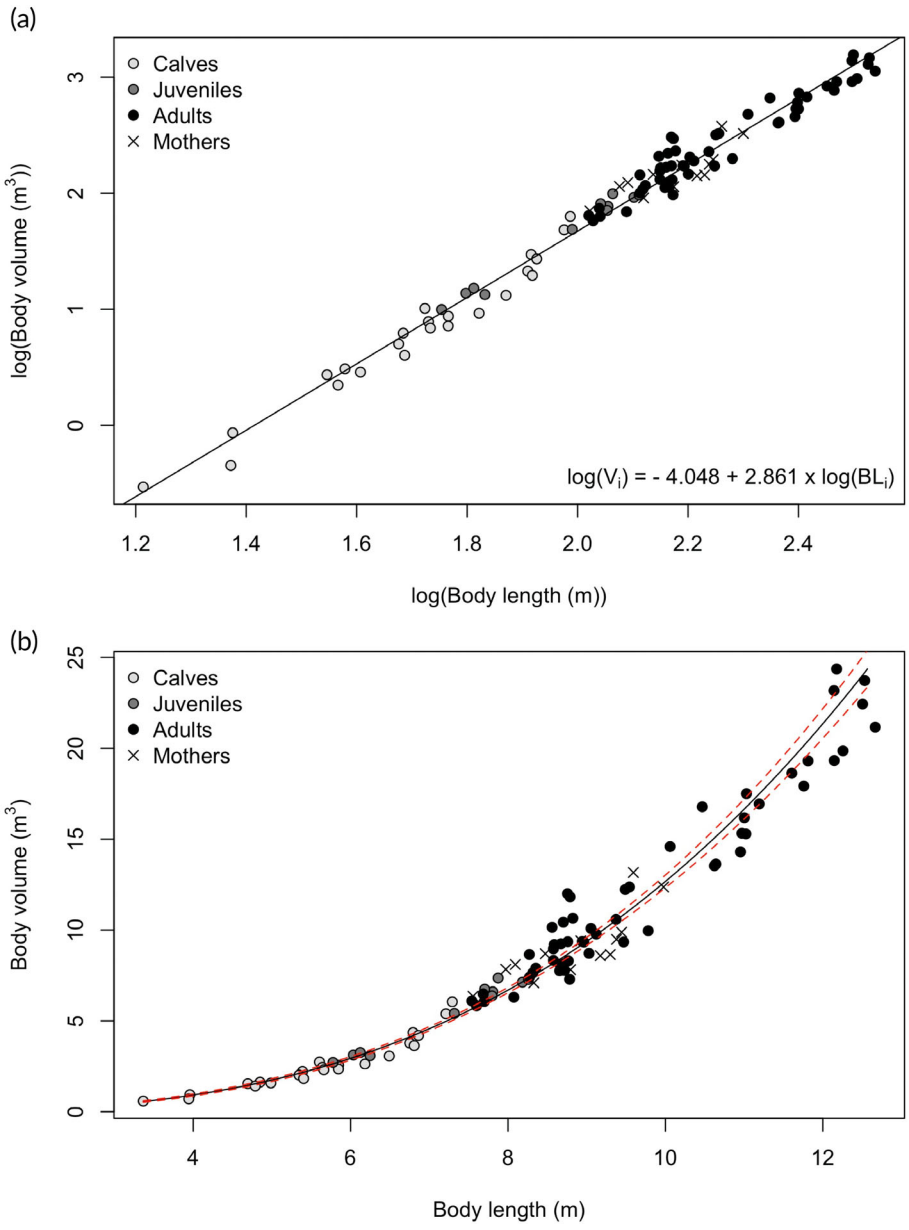

FIGURE 3 (a) Sperm whale body volume (V) estimates and body length (BL) log–log relationship for the different reproductive classes (23 calves, 11 juveniles, 55 adults and 13 mothers). The fitted regression line is represented by the solid black line. (b) Body volume (V) estimates as a function of body length (BL) for the different reproductive classes (23 calves, 11 juveniles, 55 adults and 13 mothers). The solid black line represents the back-transformed fitted values of the linear model, while the dashed red lines represent 95% confidence intervals. The data points represent the different reproductive classes (see color key).

$$\log(V_i) = -3.311 + 1.270 \times \log(BL_i) + 1.780 \times \log(G_{\text{pec},i}). \quad (16)$$

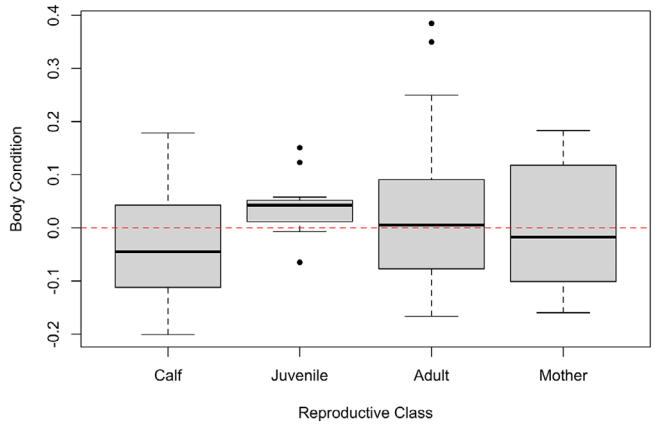

FIGURE 4 Relative body condition of individuals per reproductive class (23 calves, 11 juveniles, 55 adults, and 13 mothers). The relative body condition was calculated from the residual of the relationship between body volume and length.

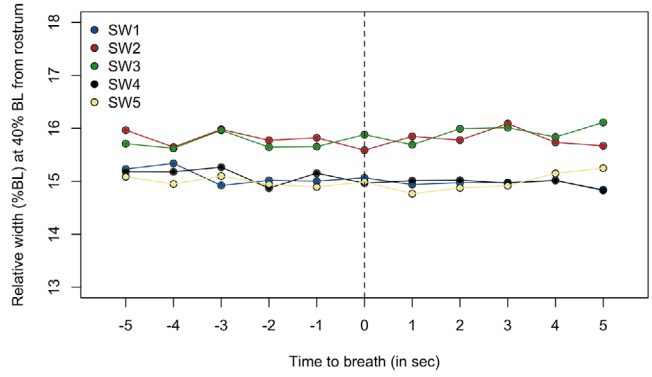

FIGURE 5 Relative width at the 40% *BL* measurement site across 1 s time intervals (before, during and after gas exchange) of sperm whales ($n = 5$). The dashed vertical line indicates the moment of exhalation. All inhalations were completed in <5 s after exhalation.

The predicted body volumes of the three dead sperm whales from the linear model were as follows: the female calf ($BL = 4.60$ m) had a body volume of 1.39 m^3, the male calf ($BL = 4.22$ m) had a body volume of 1.18 m^3, and the adult female ($BL = 11.51$ m) had a body volume of 22.11 m^3. Subsequently, their estimated average total body densities were 1,043.6, 894.7, and 695.4 kg/m^3, respectively.

3.3 | Body-mass models

Model 1. The average body density (i.e., volume-to-mass conversion factor), $D_{estimated}$, estimated using the mean body density of caught sperm whales and adjusted to include gas components, was 877.9 kg/m^3 ($SD = \pm 174.7$). Using this estimate, the predicted body mass of the free-ranging sperm whales varied from 516 to 21,390 kg ($M = 7{,}850$; $SD = 4{,}964$; Table S5, Figure 6A).

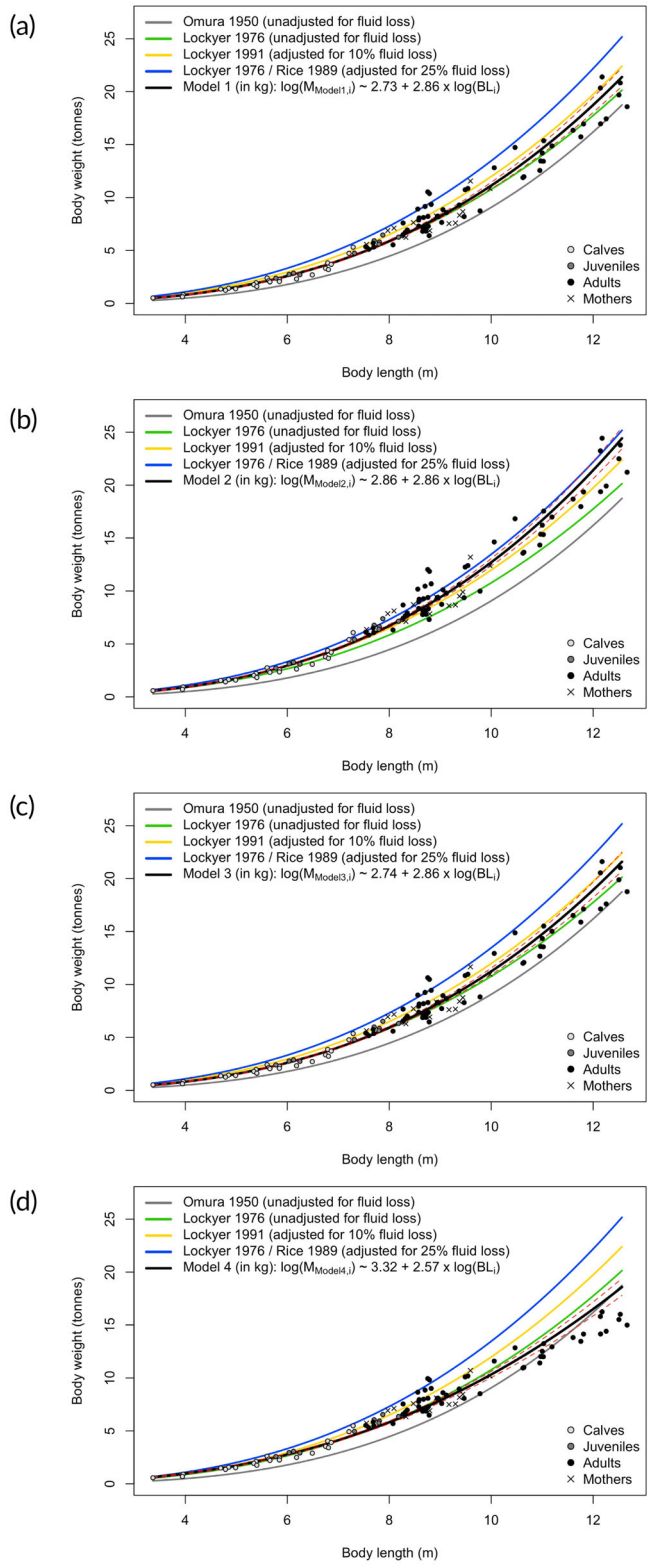

FIGURE 6 Legend on next page.

TABLE 2 Summary of all weight-length linear models (on the log–log scale) derived from the four different approaches used in this study.

Weight-length models (log–log scale)	Intercept	Slope	R^2	Matching weight-length relationship
M_1: mean cross-tissue body density deriving from whaling records	2.73	2.86	0.98	Lockyer (1976) & Lockyer (1991)
M_2: body density derived from digital tags	2.86	2.86	0.98	Lockyer (1976); Rice (1989)
M_3: mean body density based on the relative proportions of different tissue types	2.74	2.86	0.98	Lockyer (1976) & Lockyer (1991)
M_4: volume-dependent body densities	3.32	2.57	0.97	Lockyer (1976) & Omura (1950)

Model 2. The mean total body density estimate from the digital tags, D_{dtag}, recorded by Miller et al. (2004b), was 1,002.8 kg/m^3 after adjustment for gas components, and the predicted body mass of the free-ranging sperm whales varied from 589 to 24,431 kg ($M = 8{,}966$, $SD = 5{,}670$; Table S5, Figure 6B).

Model 3. The relative weight proportions of each tissue type (blubber, muscle, bones, viscera) were used in combination with tissue-specific densities (grams per millileter) to calculate the mean relative tissue density, $D_{relative}$ (Charrondiere et al., 2012; Lockyer, 1976; Lonati et al., 2019). Based on these proportions and the gas correction factor, the mean relative total tissue density, $D_{relative}$, was calculated to be 886.7 kg/m^3, and the predicted body mass of the free-ranging sperm whales varied from 521 to 21,604 kg ($M = 7{,}929$, $SD = 5{,}014$; Table S5, Figure 6C).

Model 4. The relationship between the body density of the three caught sperm whales (Lockyer, 1991) and body volume was described by the following equation:

$$D_i = 985.56 + -13.09 \times V_i. \quad (17)$$

Using this model we obtained a volume-specific conversion factor ($D_{i,estimated}$ = 666.7–977.9 kg/m^3; $M = 868.5$, $SD = 74$), and the resulting body-mass estimates of the free-ranging sperm whales varied from 575 to 16,242 kg ($M = 7{,}352$; $SD = 3{,}943$; Table S5, Figure 6D).

3.3.1 | Weight-length relationships

The relationship between predicted body mass M_i and body length BL_i for each approach is shown in Table 2, along with its model parameters and the best-matching previously published weight-length relationship (Table 2).

As expected, the residual standard errors in body mass were identical among the constant average body density models (Models 1–3, residual $SE = 0.113$), since the only variation between them was in the intercept on the log–log scale, due to the multiplication by each body density estimate (Figure S4). In contrast, the residual standard error for

FIGURE 6 Predicted body mass (M_x) of sperm whales ($n = 102$, Table S5) as a function of body length (BL). The data points represent the different reproductive classes (see color legend; 23 calves, 11 juveniles, 55 adults and 13 mothers). The solid black lines represent the predicted values from our study, where the measured body volume of free-ranging sperm whales (black points) was converted to body mass different body density values based on: (a) the mean density estimates from three caught whales (Lockyer, 1991); (b) the mean density estimate based on digital tags (Miller et al., 2004b); (c) the mean density estimated from relative tissue densities and proportions (Charrondiere et al., 2012; Lockyer, 1976, 1991; Lonati et al., 2019); and (d) volume-specific body density estimates (Lockyer, 1991). The dashed red lines represent 95% confidence intervals. The solid color lines represent the weight-length relationship reported in previously published studies (see color key).

Model 4 (residual $SE = 0.118$) differed from the other models, due to the volume-specific body density that was used to convert volume to mass for each individual (Figure S5). The sensitivity analysis showed that all model parameters were robust to measurement and scaling errors (Figure S6).

4 | DISCUSSION

This study demonstrated the feasibility of UAV photogrammetry as a noninvasive method to estimate the body mass of free-ranging sperm whales when combined with estimates of body density. Using UAV-derived measurements of body length, width and height, we were able to model the body shape of sperm whales, from which we could calculate their body volume and, ultimately, mass. The results highlighted that body volume and relative condition varied considerably in adult sperm whales, while all body-mass models were in line with existing weight estimates. Apart from providing a way to estimate body mass, this study also acts as the best current method of estimating body length of free-ranging sperm whales (Dickson et al., 2021), as it eliminates the uncertainty of extrapolating total length from other features (e.g., fluke width; Jaquet, 2006) and facilitates the fine-tuning of acoustic length estimations, which are based on the interpulse interval (IPA) of sperm whale echolocation clicks (Dickson et al., 2021; Growcott et al., 2011). Our noninvasive approach is applicable to a variety of other cetacean species and can be used to refine weight-length relationships and provide essential information on body mass in future studies of cetacean ecophysiology and bioenergetics.

To estimate body mass, we needed to obtain measurements of height and width to create a model of the sperm whale body. A few studies have attempted to describe the cross-sectional body shape of large whales, using measurements from caught or stranded animals (Lockyer et al., 1985; Sleet et al., 1981; Williamson, 1972). Other methods have used truncated cones or a cross-circular body model to describe the external morphology of cetaceans (Barratclough et al., 2014; Christiansen et al., 2018; Christiansen et al., 2020a). However, since the body of cetaceans is rarely strictly cylindrical in the cross-section, these methods may not be accurately representing the 3D shape of the body (Adamczak et al., 2019; Christiansen et al., 2019). Recent studies have demonstrated that modeling body shape as a series of infinitesimal ellipses provides a closer approximation of the body shape and volume of mysticetes (Christiansen et al., 2019; Christiansen et al., 2020b; Christiansen et al., 2021). Using this approach in the present study, we obtained height and width measurements across the body of sperm whales, which represented their cross-sectional body shape. We showed that sperm whales have a vertically elongated anterior and posterior part of their body, with a nearly 1:1 *HW* ratio across the middle part. When compared to the shape of other large whales (Christiansen et al., 2019; Christiansen et al., 2020b), the most pronounced differences seem to lie in the anterior part of their body, and specifically, around the nose area. This peculiar shape is characteristic of the external morphology of sperm whales and is attributed to the disproportionate development of their forehead, which hosts the important spermaceti organ that is used in sound production (Clarke, 1978b; Norris & Harvey, 1972).

Using our elliptical model to estimate volume, we were able to capture variations in body mass and volume in relation to body length of sperm whales, by incorporating height measurements and calculating *HW* ratios across the body axis. The mean error in body volume (and subsequent body mass) estimates of using the *HW* ratios of matching dorsal and lateral measurements to predict the *H* of dorsal-only measurements was only 5.4% ($SD = 4.53$) (Christiansen et al., 2019), which adds confidence in the accuracy of our method. Using dorsal images only (with predicted *H* from *HW* ratios), our findings suggest that body condition, volume, and subsequently body mass, fluctuates noticeably in sperm whales larger than 8 m (Figure 3). Further, the highest variation in body width (relative to *BL*) was observed between the 50% and 65% of the body for all reproductive classes (Figure S2), indicating that sperm whales may lose or gain condition mainly at this portion of their body. The blubber tissue in sperm whales is largely composed of wax esters (Koopman, 2007) and serves important functions, including thermoregulation, buoyancy, and structural roles, while also acting as an energy reserve, and hence contributes to the overall fitness of an individual (Evans et al., 2003; Lockyer, 1991). Thus, better body condition (i.e., fatter than expected for a given body

length) may be linked to increased blubber thickness, which is indicative that girth may be a good metric to assess body condition. Nonetheless, since the ecology of sperm whales does not require them to fast for prolonged periods, there is an ongoing debate as to whether and how much sperm whales can store energy as blubber, and it remains unclear how available the wax esters are as an energy source (Koopman, 2007). To what degree the morphological body condition (apparent body condition based on body shape) of sperm whales relates to their actual energy reserves (stored energy available to the whale) is hence unknown.

All our estimated mass-at-length models had strong predictive power ($R^2 > 0.97$), while the predicted body mass of sperm whales for all models was in line with existing weight measurements and weight-length relationships of previous studies (Lockyer, 1976, 1991; Ohno & Fujino, 1950; Omura, 1950). Importantly, all body-mass models accounted for the weight of body fluids, as they were based on body density estimates derived from methods that either used measurements from individuals weighed in whole (Models 1 and 4) or accounted for 14% and 25% fluid loss (Models 3 and 2, respectively). Thus, we would expect that none of our linear models would match with any of the published, uncorrected-for-fluid-loss curves. Models 3 and 4, however, were similar to the uncorrected weight-length relationships described by Lockyer (1976) and Omura (1950), respectively, indicating a slight underestimation in weight predictions deriving from these models. Model 1 provided somewhat conservative weight estimates, albeit within the range of existing body-mass measurements, similar to those of Lockyer (1991). Conversely, Model 2 allowed for a successful replicate of the weight-length curve accounting for 25% fluid loss (Lockyer, 1976; Rice, 1989) described by Miller et al. (2004b). Fluid loss during flensing has been estimated to be around 13%–15% of an animal's total mass (Gambell, 1970; Lockyer, 1991), whereas the total blood volume of sperm whales has been estimated to be 20% of its total mass (Sleet et al., 1981). Therefore, Lockyer (1991)'s 10% correction might be a conservative estimate of fluid loss, while the 25% correction of Rice (1989) used by Miller et al. (2004b) is possibly an overestimation. The slightly skewed results of our models may be attributed to these uncertainties surrounding existing body weight data of large whales (Lockyer, 1976), as well as the small sample size of whaling data on which the body density estimates for Models 1 and 4 were based (Lockyer, 1991).

We obtained similar mean body density estimates of 878 and 887 kg/m^3 for Models 1 and 3, respectively. For Model 2, we used an average body density estimate of 1,003 kg/m^3 calculated by Miller et al. (2004b) and corrected to account for gas components, who used Lockyer (1976)'s mass-at-length relationship with 25% fluid loss correction (Rice, 1989) to estimate the mass of tagged sperm whales and obtain this density estimate using a hydrodynamic model. These three estimates, however, assumed constant tissue density and did not take into account the effect of body girth and volume (i.e., body condition) on body density. In fatter animals, the percentage of total weight of muscle, bones, viscera, and fluids is relatively lower, even though the tissue-specific mass remains rather stable. Since the density of blubber is lower than other tissues (Charrondiere et al., 2012; Lonati et al., 2019), the mean body density is expected to decrease with increasing volume and vice versa. Indeed, this trend was observed in Model 4 where we used volume-dependent density as the conversion factor $D_{i,\text{estimated}} = 666.7–977.9$ kg/m^3; $M = 868.5$; $SD = 74$), highlighting the role of the relative proportion of blubber on tissue density for a given length. The only caveat of Model 4 was the very limited sample size ($n = 3$), which did not produce a significant relationship between body volume and body density, and thus led to likely inaccurate estimates for animals with higher volume, as indicated by the very low minimum density estimate of 667 kg/m^3 predicted by this model. While recognizing the statistical limitations of this approach, the conceptual idea behind it may be valuable to other researchers, as it can be applied to other species for which additional data exist.

Swimming behaviors and energetics of breath-hold divers, such as sperm whales, are directly affected by their net buoyancy, i.e., the difference between the body mass and the displaced water medium (Williams et al., 2000). All models resulted in a positively buoyant average total body density for sperm whales in seawater, which is corroborated by observations that sperm whales typically float when killed (Arregui et al., 2019; Clarke, 1978a). Our findings also align with Berzin (1972), who stated that sperm whales are positively buoyant with a mean density of 950 kg/m^3. Only few rare cases of negatively buoyant sperm whales have been reported, mostly referring to younger animals with less blubber tissue (Tønnesen et al., 2018), or to incidents when air was lost from the body due to a wound

(Berzin, 1972; Clarke, 1978a). The fact that some sperm whales sunk (i.e., became negatively buoyant) when air was removed from their body, suggests that the higher total body density (tissue and gas) value of Miller et al. (2004b), that was used in Model 2 of this study, is likely the most accurate compared to the other three models, as this is the only approach for which the tissue-only density value would be negatively buoyant. Nonetheless, the uncertainties surrounding body density estimates signify the need for more empirical measurements of densities of different tissue compartments (e.g., Lonati et al., 2019). Possible inaccuracies in the resulting body-mass predictions from our models will not affect relative metrics, such as body condition. Contrastingly, when aiming to calculate mass-specific metabolic requirements using Kleiber's equation (Kleiber, 1947), a misestimation in body density may lead to biased results. Refined methods for estimating total body density are needed to confidently predict body mass and thus, future studies need to validate existing density estimates with methods combining UAV photogrammetry and tag-derived tissue density estimates by applying both methods on the same individuals, similar to a recent study by Aoki et al. (2021). Using a combination of those two methods will enable a direct comparison and cross-validation between morphological body condition and buoyancy changes related to total lipid stores in diving cetaceans (Aoki et al., 2021).

Estimates of body mass can be used to predict mass-specific metabolic costs, as well as calculate the mass-specific costs of reproduction, locomotion, and heat loss in animals. While recognizing the uncertainties around body density estimates, obtaining noninvasive predictions of body mass of free-ranging sperm whales remains highly valuable for several ecological and physiological questions, especially given their central role in marine ecosystems (Roman et al., 2014). Our elliptical body shape model may be used to examine the influence of prey availability and infer intraseasonal or interannual changes in body condition of sperm whales in longitudinal studies (repeated sampling of the same individuals over a longer time frame). Patterns of fattening and growth in younger animals can also be detected with successive measurements over time (Christiansen et al., 2018). Finally, our approach can be used to compare the body condition of sperm whale populations exposed to different levels of environmental and anthropogenic stressors (Christiansen et al., 2020a), to aid in their management and conservation.

ACKNOWLEDGMENTS

Fieldwork in Dominica was conducted under Research Permits from the Fisheries Division of the Ministry of Agriculture, Food and Fisheries of the Government of Dominica. We thank the field team from The Dominica Sperm Whale Project. Images obtained in the Balearics were taken under administrative authorization for cetacean approaches with scientific objectives No. 13/2020 issued by MITECO. We wish to thank Fundación Biodiversidad for supporting COLCA project and all the ecovolunteers involved in the fieldwork of the Balearic Sperm Whale project. All research with sperm whales along the Hellenic Trench was conducted under the Research Permits by the Ministry of Environment & Energy (Greece) to Pelagos Cetacean Research Institute with Numbers 152931/539/2017 and ΥΠΕΝ/ΔΔΔ/3568/80 of 24/06/2020. A.F., P.A., and the Pelagos Cetacean Research Institute (PCRI) wish to thank Radamanthys Fountoulakis (Captain), Eva Papadogianni, Kostas Kostarelos, Vangelis Moschopoulos, Aggeliki Papanikita, Antonia Zirganou, Giannis Migadakis, Ermis Alexiadis, Efstathia Koitsanou, Chifundo Nyasha Michelle Ntola and Jessica Warrington for participating in the fieldwork along the Hellenic Trench. We are grateful to OceanCare (Switzerland) for their continuous support of the sperm whale research and conservation activities of the PCRI since 2008 and to Prof. Kostas Kostarelos and the University of Manchester for organizing the crowd-funding project "Nanowhales" to cofund the research expedition of 2019 along the Hellenic Trench. Lastly, we would like to thank editors Daryl Boness and Frank Fish, as well as the three anonymous reviewers for their valuable input during manuscript revision. This paper represents HIMB and SOEST contribution nos. 1903 and 11568, respectively.

AUTHOR CONTRIBUTIONS

Maria Glarou: Conceptualization; data curation; formal analysis; investigation; methodology; validation; visualization; writing – original draft; writing – review and editing. **Shane Gero:** Conceptualization; data curation; funding

acquisition; investigation; resources; writing – review and editing. **Alexandros Frantzis:** Conceptualization; data curation; funding acquisition; investigation; resources; writing – review and editing. **José María Brotons:** Conceptualization; data curation; funding acquisition; investigation; resources; writing – review and editing. **Fabien Vivier:** Data curation; investigation; writing – review and editing. **Voula Alexiadou:** Data curation; investigation; writing – review and editing. **Margalida Cerdà:** Data curation; investigation; writing – review and editing. **Enrico Pirotta:** Data curation; investigation; writing – review and editing. **Fredrik Christiansen:** Conceptualization; formal analysis; investigation; methodology; project administration; resources; supervision; validation; writing – review and editing.

COMPETING INTERESTS

No competing interests declared.

FUNDING INFORMATION

Field research in Dominica was funded through a FNU fellowship for the Danish Council for Independent Research supplemented by a Sapere Aude Research Talent Award, a Carlsberg Foundation expedition grant, a grant from Focused on Nature, and a CRE Grant from the National Geographic Society to S.G.; a FNU Large Frame Grant and Villum Foundation Grant to Peter T. Madsen at Aarhus University; and supplementary grants from the Arizona Center for Nature Conservation, Quarters For Conservation, the Dansk Akustisks Selskab, Oticon Foundation, and the Dansk Tennis Fond. Funding for data collection in the Balearics was obtained through three different projects: (1) Balearic sperm whale project, (2) Ishmael, and (3) Mares Conectados. All of them focused on investigating the sperm whale population around the Balearics and western Mediterranean waters. Project COLCA was carried out in parallel with them and was focused on obtaining remote images to quantify the occurrence of collision marks in sperm whales. This project was supported by the Fundación Biodiversidad of the Ministerio para la Transición Ecológica y Reto Demográfico of the Gobierno de España with a contribution of 70% of the funds, whereas the remaining 30% of the funds were obtained by the economic contribution of the ecovolunteers involved in the fieldwork. There was no specific funding for the estimation of sperm whale body mass (presented in this work), however the same images were used for both objectives (i.e., estimation of body mass and quantifying the collision marks). Lastly, sperm whale fieldwork along the Hellenic Trench, Greece, was funded by OceanCare (Switzerland) for both the 2019 and 2020 seasons, while the University of Manchester co-funded the 2019 fieldwork through the crowd-funding project "Nanowhales" led by Prof. Kostas Kostarelos.

ORCID

Maria Glarou https://orcid.org/0000-0002-8120-9206
Shane Gero https://orcid.org/0000-0001-6854-044X
Alexandros Frantzis https://orcid.org/0000-0001-7117-062X
Paraskevi Alexiadou https://orcid.org/0000-0003-0275-2540
Enrico Pirotta https://orcid.org/0000-0003-3541-3676
Fredrik Christiansen https://orcid.org/0000-0001-9090-8458

REFERENCES

Adamczak, S. K., Pabst, A., McLellan, W. A., & Thorne, L. H. (2019). Using 3D models to improve estimates of marine mammal size and external morphology. *Frontiers in Marine Science*, *6*, 1–12. https://doi.org/10.3389/fmars.2019.00334

Aoki, K., Isojunno, S., Bellot, C., Iwata, T., Kershaw, J., Akiyama, Y., Martín López, L. M., Ramp, C., Biuw, M., Swift, R., Wensveen, P. J., Pomeroy, P., Narazaki, T., Hall, A., Sato, K., & Miller, P. J. O. (2021). Aerial photogrammetry and tag-derived tissue density reveal patterns of lipid-store body condition of humpback whales on their feeding grounds. *Proceedings of the Royal Society B: Biological Sciences*, *288*(1943), Article 20202307. https://doi.org/10.1098/rspb.2020.2307

Arnbom, T. (1987). Individual identification of sperm whales. *Reports of the International Whaling Commission*, *37*, 201–204.

Aron, W., Burke, W., & Freeman, M. M. R. (2000). The whaling issue. *Marine Policy*, *24*(3), 179–191. https://doi.org/10.1016/S0308-597X(99)00031-7

Arregui, M., de Quirós, Y. B., Saavedra, P., Sierra, E., Suárez-Santana, C. M., Arbelo, M., Díaz-Delgado, J., Puig-Lozano, R., Andrada, M., & Fernández, A. (2019). Fat embolism and sperm whale ship strikes. *Frontiers in Marine Science*, *6*, 1–10. https://doi.org/10.3389/fmars.2019.00379

Barratclough, A., Jepson, P. D., Hamilton, P. K., Miller, C. A., Wilson, K., & Moore, M. J. (2014). How much does a swimming, underweight, entangled right whale (*Eubalaena glacialis*) weigh? Calculating the weight at sea, to facilitate accurate dosing of sedatives to enable disentanglement. *Marine Mammal Science*, *30*(4), 1589–1599. https://doi.org/10.1111/mms.12132

Berzin, A. A. (1972). *The sperm whale* [Translated from Russian]. *Israel Program for Scientific* Translations.

Booth, C. G., Sinclair, R. R., & Harwood, J. (2020). Methods for monitoring for the population consequences of disturbance in marine mammals: A Review. *Frontiers in Marine Science*, *7*, 1–18. https://doi.org/10.3389/fmars.2020.00115

Bose, N., Lien, J., & Ahia, J. (1990). Measurements of the bodies and flukes of several cetacean species. *Proceedings of the Royal Society B: Biological Sciences*, *242*(1305), 163–173. https://doi.org/10.1098/rspb.1990.0120

Burnett, J. D., Lemos, L., Barlow, D., Wing, M. G., Chandler, T., & Torres, L. G. (2019). Estimating morphometric attributes of baleen whales with photogrammetry from small UASs: A case study with blue and gray whales. *Marine Mammal Science*, *35*(1), 108–139. https://doi.org/10.1111/mms.12527

Calder, W. A. (1982). The pace of growth: An allometric approach to comparative embryonic and post embryonic growth. *Journal of Zoology*, *198*(2), 215–225. https://doi.org/10.1111/j.1469-7998.1982.tb02071.x

Cantor, M., Gero, S., Whitehead, H., & Rendell, L. E. (2019). Sperm whale: The largest toothed creature on earth. In Würsig, B. (Ed.), *Ethology and behavioral ecology of odontocetes* (pp. 261–280). Springer. https://doi.org/10.1007/978-3-030-16663-2_23 https://doi.org/https://doi.org/10.1007/978-3-030-16663-2_12

Castrillon, J., & Bengtson Nash, S. (2020). Evaluating cetacean body condition; a review of traditional approaches and new developments. *Ecology and Evolution*, *10*(12), 6144–6162. https://doi.org/10.1002/ece3.6301

Charrondiere, U. R., Haytowitz, D. B., & Stadlmayr, B. (2012). *FAO/INFOODS density database, version 2.0*. Food and Agriculture Organization of the United Nations. https://www.fao.org/3/ap815e/ap815e.pdf

Christiansen, F., Dawson, S. M., Durban, J. W., Fearnbach, H., Miller, C. A., Bejder, L., Uhart, M. M., Sironi, M., Corkeron, P., Rayment, W., Leunissen, E., Haria, E., Ward, R., Warick, H. A., Kerr, I., Lynn, M. S., Pettis, H. M., & Moore, M. J. (2020a). Population comparison of right whale body condition reveals poor state of the North Atlantic right whale. *Marine Ecology Progress Series*, *640*, 1–16. https://doi.org/10.3354/meps13299

Christiansen, F., Dujon, A. M., Sprogis, K. R., Arnould, J. P. Y., & Bejder, L. (2016). Noninvasive unmanned aerial vehicle provides estimates of the energetic cost of reproduction in humpback whales. *Ecosphere*, *7*(10), 1–18. https://doi.org/10.1002/ecs2.1468

Christiansen, F., Rodríguez-González, F., Martínez-Aguilar, S., Urbán, J., Swartz, S., Warick, H., Vivier, F., & Bejder, L. (2021). Poor body condition associated with an unusual mortality event in gray whales. *Marine Ecology Progress Series*, *658*, 237–252. https://doi.org/10.3354/meps13585

Christiansen, F., Sironi, M., Moore, M. J., Di Martino, M., Ricciardi, M., Warick, H. A., Irschick, D. J., Gutierrez, R., & Uhart, M. M. (2019). Estimating body mass of free-living whales using aerial photogrammetry and 3D volumetrics. *Methods in Ecology and Evolution*, *10*(12), 2034–2044. https://doi.org/10.1111/2041-210X.13298

Christiansen, F., Sprogis, K. R., Gross, J., Castrillon, J., Warick, H. A., Leunissen, E., & Nash, S. B. (2020b). Variation in outer blubber lipid concentration does not reflect morphological body condition in humpback whales. *Journal of Experimental Biology*, *223*(8), Article jeb213769. https://doi.org/10.1242/jeb.213769

Christiansen, F., Vivier, F., Charlton, C., Ward, R., Amerson, A., Burnell, S., & Bejder, L. (2018). Maternal body size and condition determine calf growth rates in southern right whales. *Marine Ecology Progress Series*, *592*, 267–282. https://doi.org/10.3354/meps12522

Clarke, M. R. (1972). New technique for the study of sperm whale migration. *Nature*, *238*, 405–406. https://doi.org/10.1038/238405a0

Clarke, M. R. (1978a). Buoyancy control as a function of the spermaceti organ in the sperm whale. *Journal of the Marine Biological Association of the United Kingdom*, *58*(1), 27–71. https://doi.org/10.1017/S0025315400024395

Clarke, R. (1978b). Structure and proportions of the spermaceti organ in the sperm whale. *Journal of the Marine Biological Association of the United Kingdom*, *58*(1), 1–17. https://doi.org/10.1017/S0025315400024371

Clarke, R., Paliza, O., & Van Waerebeek, K. (2011). Sperm whales of the Southeast Pacific. Part VII. Reproduction and growth in the female. *Latin American Journal of Aquatic Mammals*, *10*(1), 8–39. https://doi.org/10.5597/lajam00172

Currie, J. J., Aswegen, M. Van, Stack, S. H., West, K. L., & Vivier, F. (2021). Rapid weight loss in free ranging pygmy killer whales (*Feresa attenuata*) and the implications for anthropogenic disturbance of odontocetes. *Scientific Reports*, 1–12. https://doi.org/10.1038/s41598-021-87514-2, 8181

Dickson, T., Rayment, W., & Dawson, S. (2021). Drone photogrammetry allows refinement of acoustically derived length estimation for male sperm whales. *Marine Mammal Science*, *37*(3), 1150–1158. https://doi.org/10.1111/mms.12795

Evans, K., Hindell, M. A., & Thiele, D. (2003). Body fat and condition in sperm whales, *Physeter macrocephalus*, from southern Australian waters. *Comparative Biochemistry and Physiology Part A: Molecular & Integrative Physiology*, *134*(4), 847–862. https://doi.org/10.1016/S1095-6433(03)00045-X

Frantzis, A., Alexiadou, P., & Gkikopoulou, K. C. (2014). Sperm whale occurrence, site fidelity and population structure along the Hellenic Trench (Greece, Mediterranean Sea). *Aquatic Conservation: Marine and Freshwater Ecosystems*, *24*, 83–102. https://doi.org/10.1002/aqc.2435

Gambell, R. (1970). Weight of a sperm whale, whole and in parts. *South African Journal of Science*, *66*(7), 225–227.

Gero, S., Milligan, M., Rinaldi, C., Francis, P., Gordon, J., Carlson, C., Steffen, A., Tyack, P., Evans, P., & Whitehead, H. (2014). Behavior and social structure of the sperm whales of Dominica, West Indies. *Marine Mammal Science*, *30*(3), 905–922. https://doi.org/10.1111/mms.12086

Gero, S., & Whitehead, H. (2016). Critical decline of the eastern Caribbean sperm whale population. *PLoS ONE*, *11*(10), Article e0162019. https://doi.org/10.1371/journal.pone.0162019, 11

Goldbogen, J. A., Cade, D. E., Wisniewska, D. M., Potvin, J., Segre, P. S., Savoca, M. S., Hazen, E. L., Czapanskiy, M. F., Kahane-Rapport, S. R., DeRuiter, S. L., Gero, S., Tønnesen, P., Gough, W. T., Hanson, M. B., Holt, M. M., Jensen, F. H., Simon, M., Stimpert, A. K., Arranz, P., … Pyenson, N. D. (2019). Why whales are big but not bigger: Physiological drivers and ecological limits in the age of ocean giants. *Science*, *366*, 1367–1372. https://doi.org/10.1126/science.aax9044

Goldbogen, J. A., & Madsen, P. T. (2018). The evolution of foraging capacity and gigantism in cetaceans. *Journal of Experimental Biology*, *221*(11), Article jeb166033. https://doi.org/10.1242/jeb.166033

Green, A. J. (2001). Mass/length residuals: Measures of body condition or generators of spurious results? *Ecology*, *82*(5), 1473–1483. https://doi.org/10.1890/0012-9658(2001)082[1473:MLRMOB]2.0.CO;2

Growcott, A., Miller, B., Sirguey, P., Slooten, E., & Dawson, S. (2011). Measuring body length of male sperm whales from their clicks: The relationship between inter-pulse intervals and photogrammetrically measured lengths. *Journal of the Acoustical Society of America*, *130*(1), 568–573. https://doi.org/10.1121/1.3578455

Irvine, L. G., Thums, M., Hanson, C. E., McMahon, C. R., & Hindell, M. A. (2017). Quantifying the energy stores of capital breeding humpback whales and income breeding sperm whales using historical whaling records. *Royal Society Open Science*, *4*(3). https://doi.org/10.1098/rsos.160290

Irving, L., Scholander, P. F., & Grinnell, S. W. (1941). The respiration of the porpoise, *Tursiops truncatus*. *Journal of Cellular and Comparative Physiology*, *17*(2), 145–168. https://doi.org/10.1002/jcp.1030170203

Jakob, E. M., Marshall, S. D., & Uetz, G. W. (1996). Estimating fitness: A comparison of body condition indices. *Oikos*, *77*, 61–67. https://doi.org/10.2307/3545585

Jaquet, N. (2006). A simple photogrammetric technique to measure sperm whales at sea. *Marine Mammal Science*, *22*(4), 862–879. https://doi.org/10.1111/j.1748-7692.2006.00060.x

Jauniaux, T., Brosens, L., Smeenk, C., Jacquinet, E., Lambrights, D., Addink, M., & Coignoul, F. (1998). Postmortem investigations on winter stranded sperm whales from the coasts of Belgium and the Netherlands. *Journal of Wildlife Diseases*, *34*(1), 99–109. https://doi.org/10.7589/0090-3558-34.1.99

Jensen, F. H., Johnson, M., Ladegaard, M., Wisniewska, D. M., & Madsen, P. T. (2018). Narrow acoustic field of view drives frequency scaling in toothed whale biosonar. *Current Biology*, *28*(23), 3878-3885.e3. https://doi.org/10.1016/j.cub.2018.10.037

Jiang, W. Bin, Han, J., Ma, X. W., Liu, H., Yu, S. B., & Sui, H. J. (2021). Plastination of a sperm whale. *Journal of Anatomy*, *240*, 669–677. https://doi.org/10.1111/joa.13581

Kleiber, M. (1947). Body size and metabolic rate. *Physiological Reviews*, *27*(4), 512–541. https://doi.org/10.1152/physrev.1947.27.4.511

Koopman, H. N. (2007). Phylogenetic, ecological, and ontogenetic factors influencing the biochemical structure of the blubber of odontocetes. *Marine Biology*, *151*(1), 277–291. https://doi.org/10.1007/s00227-006-0489-8

Kooyman, G. L., Castellini, M. A., & Davis, R. W. (1981). Physiology of diving in marine mammals. *Annual Review of Physiology*, *43*, 343–356. https://doi.org/10.1146/annurev.ph.43.030181.002015

Laurie, A. H. (1933). Some aspects of respiration in blue and fin whales. *Discovery Reports*, *7*, 365–406.

Lavery, T. J., Roudnew, B., Gill, P., Seymour, J., Seuront, L., Johnson, G., Mitchell, J. G., & Smetacek, V. (2010). Iron defecation by sperm whales stimulates carbon export in the Southern Ocean. *Proceedings of the Royal Society B: Biological Sciences*, *277*, 3527–3531. https://doi.org/10.1098/rspb.2010.0863

Lockyer, C. (1976). Body weights of some species of large whales. *ICES Journal of Marine Science*, *36*(3), 259–273. https://doi.org/10.1093/icesjms/36.3.259

Lockyer, C. (1981). Estimates of growth and energy budget for the sperm whale, *Physeter catodon*. In *Mammals in the seas* (Vol. III, pp. 489–504). FAO Series No. 5.

Lockyer, C. (1991). Body composition of the sperm whale, Physeter catodon, with special reference to the possible functions of fat depots. *Journal of the Marine Research Institute, Reykjavik*, *12*(2), 1–25.

Lockyer, C. H., McConnell, L. C., & Waters, T. D. (1985). Body condition in terms of anatomical and biochemical assessment of body fat in North Atlantic fin and sei whales. *Canadian Journal of Zoology*, *63*(10), 2328–2338. https://doi.org/10.1139/z85-345

Lonati, G. L., Singleton, E. M., Phelps, C. E., Koopman, H. N., & Pabst, D. A. (2019). The density of odontocete integument depends on blubber lipid composition and temperature. *Marine Mammal Science*, *35*(2), 595–616. https://doi.org/10.1111/mms.12554

McClain, C. R., Balk, M. A., Benfield, M. C., Branch, T. A., Chen, C., Cosgrove, J., Dove, A. D. M., Gaskins, L., Helm, R. R., Hochberg, F. G., Lee, F. B., Marshall, A., McMurray, S. E., Schanche, C., Stone, S. N., & Thaler, A. D. (2015). Sizing ocean giants: patterns of intraspecific size variation in marine megafauna. *PeerJ*, *3*, Article e715. https://doi.org/10.7717/peerj.715

McNab, B. (1963). Bioenergetics and the determination of home range size. *American Naturalist*, *97*(894), 133–140. https://doi.org/10.1086/282264

Miller, P. J. O., Johnson, M. P., & Tyack, P. L. (2004a). Sperm whale behaviour indicates the use of echolocation click buzzes "creaks" in prey capture. *Proceedings of the Royal Society B: Biological Sciences*, *271*, 2239–2247. https://doi.org/10.1098/rspb.2004.2863

Miller, P. J. O., Johnson, M. P., Tyack, P. L., & Terray, E. A. (2004b). Swimming gaits, passive drag and buoyancy of diving sperm whales *Physeter macrocephalus*. *Journal of Experimental Biology*, *207*(11), 1953–1967. https://doi.org/10.1242/jeb.00993

Moore, J. E., & Read, A. J. (2008). A Bayesian uncertainty analysis of cetacean demography and bycatch mortality using age-at-death data. *Ecological Applications*, *18*(8), 1914–1931. https://doi.org/10.1890/07-0862.1

Moore, M. J., Knowlton, A., Kraus, S. D., McLellan, W. A., & Bonde, R. K. (2004). Morphometry, gross morphology and available histopathology in North Atlantic right whale (*Eubalaena glacialis*) mortalities. *Journal of Cetacean Research and Management*, *6*(3), 199–214.

Moya-Laraño, J., Macías-Ordóñez, R., Blanckenhorn, W. U., & Fernández-Montraveta, C. (2008). Analysing body condition: Mass, volume or density? *Journal of Animal Ecology*, *77*(6), 1099–1108. https://doi.org/10.1111/j.1365-2656.2008.01433.x

Nishiwaki, M., Ohsumi, S., & Maeda, Y. (1963). Change of form in the sperm whale accompanied with growth. *Scientific Report of the Whales Research Institute, Tokyo*, *17*, 1–14. https://doi.org/10.1016/0011-7471(65)91505-6

Norris, K. S., & Harvey, G. W. (1972). A theory for the function of the spermaceti organ of the sperm whale (*Physeter catodon* L.). *Animal Orientation and Navigation*, (Special Publication 262), 393–417.

Notarbartolo di Sciara, G., Frantzis, A., Bearzi, G., & Reeves, R. (2012). *Physeter macrocephalus* (Mediterranean subpopulation). *IUCN Red List of Threatened Species*, e.T1637073. https://doi.org/https://doi.org/10.2305/IUCN.UK.2012-1.RLTS.T16370739A16370477.en

Ohno, M., & Fujino, K. (1950). Biological investigation on the whales caught by the Japanese Antarctic whaling fleets, season 1950-51. *Scientific Reports of the Whales Research Institute, Tokyo*, *7*, 125–190.

Olsen, C. R., Hale, F. C., & Elsner, R. (1969). Mechanics of ventilation in the pilot whale. *Respiration Physiology*, *7*(2), 137–149. https://doi.org/10.1016/0034-5687(69)90001-2

Omura, H. (1950). On the body weight of sperm and sei whales located in the adjacent waters of Japan. *Scientific Reports of the Whales Research Institute, Tokyo*, *4*, 1–13.

Peig, J., & Green, A. J. (2010). The paradigm of body condition: A critical reappraisal of current methods based on mass and length. *Functional Ecology*, *24*(6), 1323–1332. https://doi.org/10.1111/j.1365-2435.2010.01751.x

Porter, W. P., & Kearney, M. (2009). Size, shape, and the thermal niche of endotherms. *Proceedings of the National Academy of Sciences of the United States of America*, *106*, 19666–19672. https://doi.org/10.1073/pnas.0907321106

R Development Core Team. (2018). *R: A language and environment for statistical computing* [Computer software]. R Foundation for Statistical Computing.

Rice, D. W. (1989). Sperm whale *Physeter macrocephalus* Linnaeus, 1758. In S. H. Ridgway (Ed.) *Handbook of marine mammals* (Vol. 4, pp. 177–233). Academic Press.

Roman, J., Estes, J. A., Morissette, L., Smith, C., Costa, D., McCarthy, J., Nation, J. B., Nicol, S., Pershing, A., & Smetacek, V. (2014). Whales as marine ecosystem engineers. *Frontiers in Ecology and the Environment*, *12*(7), 377–385. https://doi.org/10.1890/130220

Roman, J., & McCarthy, J. J. (2010). The whale pump: Marine mammals enhance primary productivity in a coastal basin. *PLoS ONE*, *5*(10), Article 13255. https://doi.org/10.1371/journal.pone.0013255

Schmidt-Nielsen, K. (1984). *Scaling: Why is animal size so important?* Cambridge University Press.

Sleet, R. B., Sumich, J. L., & Weber, L. J. (1981). Estimates of total blood volume and total body weight of a sperm whale (*Physeter catodon*). *Canadian Journal of Zoology*, *59*(3), 567–570. https://doi.org/10.1139/z81-083

Smith, C. R. (2007). Bigger is better: The role of whales as detritus in marine ecosystems. In J. A. Estes (Ed.), *Whales, whaling, and ocean ecosystems* (pp. 286–300). University of California Press. https://doi.org/10.1525/9780520933200-026

Soulsbury, C. D. (2019). Income and capital breeding in males: Energetic and physiological limitations on male mating strategies. *Journal of Experimental Biology*, *222*(1), Article jeb184895. https://doi.org/10.1242/jeb.184895

Stephens, P. A., Boyd, I. L., McNamara, J. M., & Houston, A. I. (2009). Capital breeding and income breeding; their meaning, measurement, and worth. *Ecology*, *90*(8), 2057–2067. https://doi.org/10.1890/08-1369.1

Stevenson, R. D., & Woods, W. A. (2006). Condition indices for conservation: New uses for evolving tools. *Integrative and Comparative Biology*, *46*(6), 1169–1190. https://doi.org/10.1093/icb/icl052

Taylor, B. L., Baird, R., Barlow, J., Dawson, S. M., Ford, J., Mead, J. G., Notarbartolo di Sciara, G., Wade, P., & Pitman, R. L. (2019). *Physeter macrocephalus*. *IUCN Red List of Threatened Species*, *e.T41755A1*. https://doi.org/https://doi.org/10.2305/IUCN.UK.2008.RLTS.T41755A160983555.en

Tomilin, A. G. (1967). *Mammals of the USSR and adjacent countries - Cetacea* [Translated from Russian]. Israel Program for Scientific Translations, Jerusalem.

Tønnesen, P., Gero, S., Ladegaard, M., Johnson, M., & Madsen, P. T. (2018). First-year sperm whale calves echolocate and perform long, deep dives. *Behavioral Ecology and Sociobiology*, *72*(10), Article 165. https://doi.org/10.1007/s00265-018-2570-y

Tønnesen, P., Oliveira, C., Johnson, M., & Madsen, P. T. (2020). The long-range echo scene of the sperm whale biosonar. *Biology Letters*, *16*(8), Article 20200134. https://doi.org/10.1098/rsbl.2020.0134

Villegas-Amtmann, S., Schwarz, L. K., Sumich, J. L., Costa, D. P., & Peters, D. P. C. (2015). A bioenergetics model to evaluate demographic consequences of disturbance in marine mammals applied to gray whales. *Ecosphere*, *6*(10), Article 183. https://doi.org/10.1890/ES15-00146.1

Watwood, S. L., Miller, P. J. O., Johnson, M., Madsen, P. T., & Tyack, P. L. (2006). Deep-diving foraging behaviour of sperm whales (*Physeter macrocephalus*). *Journal of Animal Ecology*, *75*(3), 814–825. https://doi.org/10.1111/j.1365-2656.2006.01101.x

Whitehead, H. (2002). Estimates of the current global population size and historical trajectory for sperm whales. *Marine Ecology Progress Series*, *242*, 295–304. https://doi.org/10.3354/meps242295

Whitehead, H. (2003). *Sperm whales: Social evolution in the ocean*. University of Chicago Press.

Whitehead, H., & Gordon, J. (1986). Methods of obtaining data for assessing and modeling populations of sperm whales which do not depend on catches. *Reports of the International Whaling Commission*, *8*, 149–166.

Williams, T. M., Davis, R. W., Fuiman, L. A., Francis, J., Le Boeuf, B. J., Horning, M., Calambokidis, J., & Croll, D. A. (2000). Sink or swim: Strategies for cost-efficient diving by marine mammals. *Science*, *288*(5463), 133–136. https://doi.org/10.1126/science.288.5463.133

Williamson, G. R. (1972). The true body shape of rorqual whales. *Journal of Zoology*, *167*(3), 277–286. https://doi.org/10.1111/j.1469-7998.1972.tb03111.x

SUPPORTING INFORMATION

Additional supporting information can be found online in the Supporting Information section at the end of this article.

How to cite this article: Glarou, M., Gero, S., Frantzis, A., Brotons, J. M., Vivier, F., Alexiadou, P., Cerdà, M., Pirotta, E., & Christiansen, F. (2022). Estimating body mass of sperm whales from aerial photographs. *Marine Mammal Science*, 1–23. https://doi.org/10.1111/mms.12982